

# Tunable photonic performance of three-dimensional macroporous tungsten oxide

DENGTENG GE<sup>b</sup>, YANBO DING<sup>c</sup>, ZHONGQIU TONG<sup>b</sup>, WUHONG XIN<sup>b</sup>, ZHENYU LI<sup>b</sup>, LILI YANG<sup>a,\*</sup>

<sup>a</sup>*School of Transportation Science and Engineering, Harbin Institute of Technology, Harbin, 150090, P.R. China*

<sup>b</sup>*Center for Composite Materials and Structures, Harbin Institute of Technology, Harbin, 150080, P.R. China*

<sup>c</sup>*School of Chemical Engineering and Technology, Harbin Institute of Technology, Harbin, 150001, P.R. China*

Electrochromic materials with photonic crystal structures attract enormous interest and have potential applications as smart thermal control coatings due to the tunable optical switching performance. Here we report tungsten oxides ( $\text{WO}_3$ ) films with three-dimensional macroporous structures electrochemically fabricated through polystyrene (PS) colloidal crystal templates. Their switching photonic performance through electrochromic process was studied experimentally and theoretically. UV-Vis-NIR spectra of  $\text{WO}_3/\text{PS}$  photonic crystals show that abnormal red shift of band gap occurs during the infiltrated of tungsten oxide or the bleaching process. It is deduced that the switching of photonic performance is weakened due to the absorption of infiltrated tungsten oxide. An effective fraction of materials involved in the Bragg effect  $\phi_{\text{trans}}$  was introduced here to describe the effect of absorption on the photonic structures. It is obtained that 60% of  $\text{WO}_3$  in tungsten oxide electrochromic photonic crystals are involved due to their absorption.

(Received May 16, 2012; accepted September 20, 2012)

*Keywords:* Tungsten oxide, Tunable photonic crystals, Absorption, Electrochromic

## 1. Introduction

Photonic crystals (PhC) have shown their potential applications in photoelectric device, lasers, optical communication systems because of their controllability and manipulation of the propagation of electromagnetic waves or lights [1-5]. Tunable photonic crystals is definitely a big challenge and innovation to switch the photonic band performance, which provides application prospects in chemical and biology sensors, optical interconnects et al [6-8]. Typical ways are to change the lattice spacing or the dielectric constants of PhC materials through outer fields or addition of other materials [9-12]. Electrochromic materials could change their optical properties continuously and reversibly by electric fields. As excellent inorganic electrochromic materials, tungsten oxide ( $\text{WO}_3$ ) has been of great interest due to their chemical stability, excellent resistance to radiation and high temperatures [13, 14]. Tungsten oxide films tune their transparency easily by the ion-intercalation/extraction reaction in the presence of a small electric potential difference [15]. Three-dimensional ordered macroporous (3DOM) tungsten oxide were prepared by Sumida and Kuai et al, and it is found that the band gap of 3DOM  $\text{WO}_3$  had a shift in visible band during the coloration/bleaching process [16, 17]. Interesting optical properties of 3DOM  $\text{WO}_3$  prepared through sol-gel method were also found in the infrared region [18, 19]. However, the tunable photonic performance was simply described in terms of refractive index change of tungsten oxide during the electrochromic process. In our previous research, it has been proved that the photonic performance of metallic photonic crystals

would be greatly affected by the absorption of materials [20]. In this work, tungsten oxide photonic crystals with different lattice spacing were electrochemically deposited and their tunable photonic properties were studied both from the real and imaginary part of dielectric constant. A suppression of tunable photonic performance is found because of the existence of absorption.

## 2. Materials and methods

### 2.1 Fabrication of templates

Monodispersed polystyrene (PS) spheres with relative standard deviation smaller than 5% (on the diameter) were obtained using an emulsifier-free emulsion polymerization technique [21]. Three sizes of PS spheres were chosen to form templates. Fluorine-doped tin oxides (FTO) glass slides were used as the substrates for PS template growth. PS colloidal crystals with 20~30 layers spheres were grown using a controlled vertical drying method [22]. However, there are still few defects for the colloidal crystals with average uniform area of  $10 \times 10 \mu\text{m}^2$ .

### 2.2 Preparation of tungsten oxide photonic crystals

The electrolyte solution was prepared as follows: 5.16 g of sodium tungstate ( $\text{Na}_2\text{WO}_4$ ) was dissolved in 25 ml 30%  $\text{H}_2\text{O}_2$ . The excess  $\text{H}_2\text{O}_2$  was decomposed by putting a large area Pt sheet into the solution until  $\text{O}_2$  gas evolution had stopped. Finally the solution was diluted to 0.25 M and  $\text{pH}=7\sim 8$  with 70/30 v/v water/isopropanol.

The electrochemical setup was performed on CHI 600D (CH Instrument Co. Ltd.). FTO glass coated with PS opal photonic crystals were used as work electrode. Pt sheet was used as the counter electrode and the reference electrode was Ag/AgCl electrode in 4M KCl saturated with AgCl. The electrodeposition was carried out under a current density of 0.2 A/dm<sup>2</sup> for 180 second. The resulting films were thoroughly washed with deionized water and ethanol for the removal of surfactant and dried in air.

### 2.3 Characterization

The coloring/bleaching process was performed in an electrolyte solution (1 M LiClO<sub>4</sub> in propylene carbonate) between +1.5 and -1.5 V. The WO<sub>3</sub>/PS composite films were used as working electrode. Pt foil was used as the counter electrode and Ag/AgCl as the reference electrode. The reflection spectra were obtained from Ocean Maya 2000-Pro UV-Vis-NIR fiber optic spectrometer. The incident light was perpendicular to the surface of samples.

Scanning electron microscopy (QUANTA 200F, FEI, America) was performed to give surface morphology. A Hitachi H-7650 transmission electronic microscopy (TEM) was used to study the microstructure. The ultra small angle X-ray scattering (USAXS) experiments were carried on the 1W2A beamline at Beijing Synchrotron Radiation Facility (BSRF) using wavelength of 0.154 nm. The distance between the CCD and sample  $D_s$  is 4.85m.

## 3. Results and discussions

The top-viewed SEM image of PS templates with three kinds of lattice spacing is shown in Fig. 1. It reveals a good ordering close packed array of PS templates. Through direct measurement, the center-to-center distance of PS spheres  $D$  are 220 nm, 308 nm, 400 nm, respectively. To evaluate the ordered structure over the whole sample, small angle X-ray scattering pattern of alloy/PS PCs with lattice size of 220 nm sphere is shown in Fig. 2. The sharp Bragg speckles suggests that a single-crystal domain of fcc structure is irradiated by the X-ray beam. With the comparison of scattering speckles' distance from center of scattering, the scattering pattern can be indexed. For an fcc lattice  $q$  values of each crystalline diffraction plane ( $q_{hkl}$ ) are calculated from [23]:

$$q = \frac{2\pi}{d_{hkl}} = \frac{\sqrt{2}\pi}{D} \sqrt{(h^2 + k^2 + l^2)} \quad (1)$$

where  $d_{hkl}$  is the interplanar spacing between ( $h k l$ ) planes. The  $q$  value of the speckles can be easily obtained 0.058 nm<sup>-1</sup> from Fit 2D software. With the comparison of SEM result,  $D$  can be calculated to be 214 nm and the speckles were indexed. The sharp diffraction speckles result from the Bragg diffraction on (220) crystallographic plane. Therefore, there is a good stability of ordered structure of templates during the infiltration of tungsten oxide. Fig. 3 shows the SEM and TEM images of tungsten oxide films.

It can be seen that the films are made up of spherical grains of the order of 10 nm and these grains are in good contact with each other. Some nano-pores were also shown in the micrographs of films.

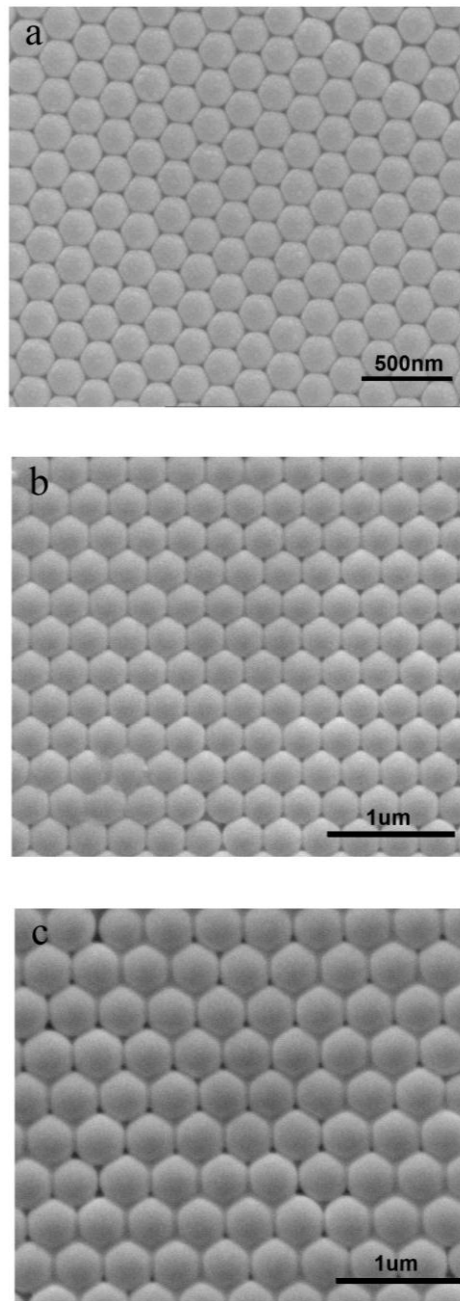


Fig. 1. SEM images of PS templates with three different lattice spacing.

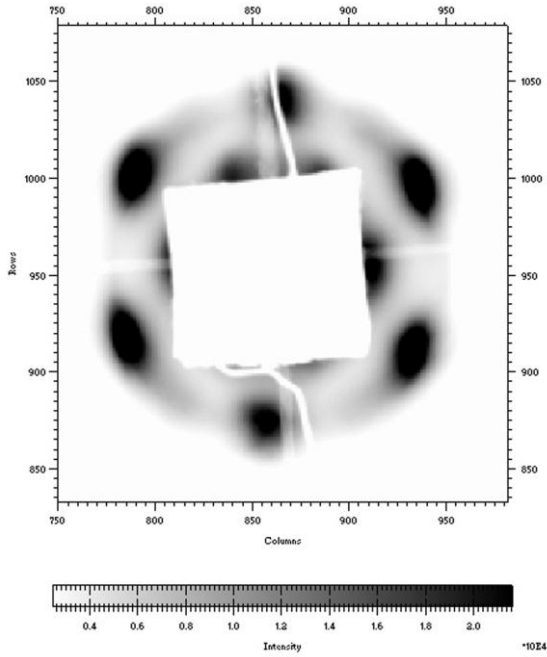


Fig. 2. SAXS pattern of PS template with a lattice size of 220 nm.

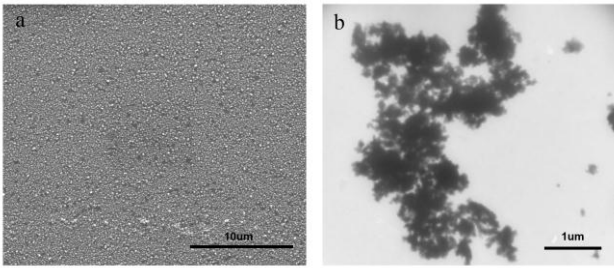


Fig. 3. SEM (a) and TEM (b) photographs of electrodeposited tungsten oxide films.

Fig. 4 shows the UV-Vis-NIR reflective spectra of PS templates, colored and bleached  $\text{WO}_3/\text{PS}$  composite photonic crystals with the lattice spacing of 220 nm, 308 nm and 400 nm. It is obvious that all curves reveal pronounced reflectance peaks arising from the destructive interference effect between reflections off the layers of ordered structure. Distinct red shift of the position of band stop can be observed from PS templates to colored  $\text{WO}_3/\text{PS}$  composites then to bleached materials. Compared with the position of photonic bandgap of PS templates, a red shift value of 25 nm, 10 nm and 16 nm is observed due to the infiltration of tungsten oxide and ion-intercalation, respectively. While a red shift of 5 nm, 36 nm, 62 nm is present due to the bleaching process. These phenomena are originally related with interaction between lights and materials, while Bragg-Snell's law has been widely used to explain it. According to the Bragg's law, i.e., the position of band gap can be calculated from [25]:

$$\lambda_{\max} = 2d \cdot (n_{\text{eff}}^2 - \sin^2 \theta)^{1/2} \quad (2)$$

where  $d$ ,  $n_{\text{eff}}$ ,  $\theta$  represent the interplanar spacing, the effective refractive index and the incidence angle against the normal direction.  $n_{\text{eff}}$  usually is given by the Snell's law as follows:

$$n_{\text{eff}} = n_{\text{sphere}} f_{\text{sphere}} + n_{\text{fill}} f_{\text{fill}} \quad (3)$$

where  $n$ ,  $f$  are the refractive index of materials and each volume ratio. From the Bragg-Snell's law, it is deduced that the position of photonic bandgap is proportional to the lattice spacing under the condition of fixed materials and incidental angle. The tested results obviously show that the photonic performance of tungsten oxide PhC is not in line with the Bragg-Snell's law.

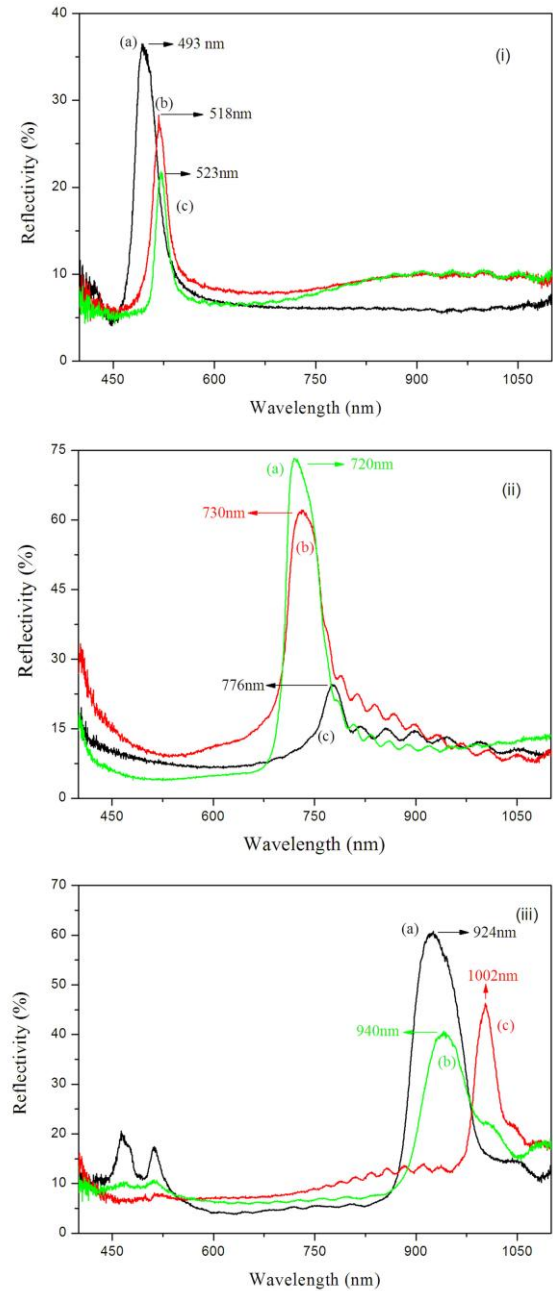
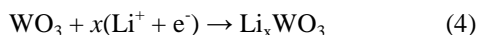


Fig. 4. UV-Vis-NIR spectra of PS templates (a) and  $\text{WO}_3/\text{PS}$  composite photonic crystals at colored (b) and bleached (c) states with lattice spacing of (i) 220 nm, (ii) 308 nm and (iii) 400 nm.

As well known, the electrochromic performance of tungsten oxide originally results from the injection and extraction of electrons and ions. The general equation can be written as:



It is pointed that the refractive index of  $\text{WO}_3$  is 1.75 and that of  $\text{LiWO}_3$  is 1.49. According to the Bragg-Snell's law, the position of bandgap of PS templates or colored PS/ $\text{WO}_3$  or bleached PS/ $\text{WO}_3$  would be in proportion to the lattice spacing. However, it's not true here. Therefore, both the refraction and the absorption of materials should be under consideration during the analysis of tunable photonic performance of PS/ $\text{WO}_3$ , namely, both the real and imaginary parts of dielectric constant.

As a result of absorption of tungsten oxide materials, the volume of infiltrated materials through which lights can penetrate is decreased, i.e., just part of materials is participating in the Bragg interference. The depth of infiltrated materials through which lights can transmit will also be decreased, i.e., the layers of lattice will be decreased. The former one results in the deviation of Bragg-Snell's law, while the latter one causes the decrease of intensity of Bragg reflective peak. To describe the effect of absorption of infiltrated materials on their photonic performance quantitatively, the effective fraction of infiltrated tungsten oxide  $\varphi_{\text{trans}}$  was also introduced here and then equation (3) is transformed into:

$$n_{\text{eff}} = n_{\text{sphere}} \cdot f_{\text{sphere}} + n_{\text{alloy}} \cdot f_{\text{alloy}} \cdot \varphi_{\text{trans}} \quad (5)$$

Through the equation (5), the effective fraction  $\varphi_{\text{trans}}$  can be obtained 67%, 58% and 60% for colored  $\text{WO}_3/\text{PS}$  composites and 56%, 59% and 60% for discolored composites with the increase of PS diameter. It is deduced that 60% of tungsten oxide can be considered as transmission medium of lights and participate in the Bragg effects while 40% can be treated as the "black-hole" of lights approximately.

#### 4. Conclusions

Tungsten oxide photonic crystals were prepared through colloidal template-assisted electrodeposition method. The switching photonic performance of  $\text{WO}_3/\text{PS}$  composite was studied during the coloration/bleaching process. A red shift of position of band gap was found during the infiltration of tungsten oxide or the bleaching process. From the analysis in terms of real and imaginary part of dielectric constant of materials, an effective fraction of involved tungsten oxide  $\varphi_{\text{trans}}$  was introduced to quantitatively describe the influence of absorption. It is deduced that the switching photonic performance of electrochromic photonic crystals is weakened because of the absorption of infiltrated materials and  $\varphi_{\text{trans}}=60\%$  was obtained for tungsten oxide photonic crystals. The studies on the photonic performance can effectively help understanding the optical switching properties of tunable photonic crystals.

#### Acknowledgements

The authors gratefully acknowledge Prof. Zhonghua Wu and his team for their help in carrying out the SAXS experiments at Institute of High Energy Physics, Beijing, China. This work is supported by the Program National Natural Science Foundation (No. 51102068) and the Fundamental Research Funds for the Central Universities (Grant No. HIT.NSRIF.2010034).

#### References

- [1] J. D. Joannopoulos, P. R. Villeneuve, S. Fan, *Nature* **386**, 143 (1997).
- [2] K. Lee, S. A. Asher, *J. Am. Chem. Soc.* **122**, 9534 (2000).
- [3] J. H. Holtz, S. A. Asher, *Nature* **389**, 829 (1997).
- [4] T. Cassagneau, F. Caruso, *Adv. Mater.* **14**, 1629 (2002).
- [5] S. John, T. Quang, *Phys. Rev. Lett.* **74**, 3419 (1995).
- [6] S. M. Weiss, M. Haurylau, P. M. Fauchet, *Opt. Mater.* **27**(5), 740 (2005).
- [7] R. V. Nair, R. Vijaya, *Opt. Mater.* **32**(2), 387 (2009).
- [8] S. W. Leonard, J. P. Mondia, H. M. van Driel, et al. Lehmann, *Phys. Rev. B* **61**, 2389 (2000).
- [9] T. S. Deng, J. Y. Zhang, K. T. Zhu, *Opt. Mater.* **32**(9), 946 (2010).
- [10] K. Shimazaki, S. Tachikawa, et al. *Int. J. Thermophys.* **22**(5), 1549 (2001).
- [11] M. Ozaki, Y. Shimoda, M. Kasano, et al. *Adv. Mater.* **14**(7), 514 (2002).
- [12] J. Q. Xia, Y. R. Ying, S. H. Foulger, *Adv. Mater.* **17**, 2463 (2005).
- [13] K. Bange, T. Gambke, *Adv. Mater.* **2**, 10 (1990).
- [14] S. T. Wang, X. J. Feng, J. N. Yao, L. Jiang, *Angew. Chem. Int. Ed.* **45**, 1264 (2006).
- [15] A. Azens, A. Hjelm, D. L. Bellac, et al, *Solid State Ionics* **86-88**, 943 (1996).
- [16] T. Sumida, Y. Wada, T. Kitamura, S. Yanagida, *Chem. Lett.* (2), 180 (2002).
- [17] S. L. Kuai, G. Bader, P. V. Ashrit, *Appl. Phys. Lett.* **86**, 221110 (2005).
- [18] M. Sadakane, K. Sasaki, H. Kunioku, B. Ohtani, R. Abe, W. Ueda, *J. Mater. Chem.* **20**, 1811 (2010).
- [19] S. Badilescu, P. V. Ashrit, *Solid State Ionics* **158**, 187 (2003).
- [20] D. T. Ge, L. L. Yang, Y. Li, J. P. Zhao, X. Li, H. J. Zhao, *Synth. Met.* **161**, 235 (2011).
- [21] M. A. Mclachlan, N. P. Johnson, R. M. Rue La De, D. W. McComb, *J. Mater. Chem.*, **14**, 144 (2004).
- [22] C. J. Brinker, Y. F. Lu, A. Sellinger, H. Y. Fan, *Adv. Mater.* **11**(7), 579 (1999).
- [23] S. S. Hu, Y. F. Men, S. V. Roth, R. Gehrke, J. Rieger, *Langmuir* **24**, 1620 (2008).
- [24] I. Shiyonovskaya, M. Hepel, E. Tewksbury, *J. New Mater. Electrochem. Syst.* **3**, 241 (2000).
- [25] R. C. Schroden, M. Al-Daous, C. F. Blanford, A. Stein, *Chem. Mater.* **14**, 3305 (2002).

\*Corresponding author: liliyang@hit.edu.cn